IEEE Transactions on Nuclear Science, Vol. NS-26, No. 3, June 1979

A SUPERCONDUCTING HIGH-LUMINOSITY INSERTION IN THE INTERSECTING STORAGE RINGS (ISR)

J. Billan, K.N. Henrichsen, H. Laeger, Ph. Lebrun, R. Perin, S. Pichler, P. Pugin, L. Resegotti, P. Rohmig, T. Tortschanoff, A. Verdier, L. Walckiers, R. Wolf

Abstract

A focusing insertion will be constructed at an intersection of the ISR, to achieve a reduction of the effective beam height by about a factor 6 in the interaction diamond and a corresponding increase of the luminosity. It will contain eight superconducting quadrupole magnets, capable of producing gradients of 43 $T\,m^{-1}$ in a warm bore of 173 mm diameter: four of them have a magnetic length of 1.15 m and four of 0.65 m. The magnets are also equipped with sextupole windings, to match the gradients to particle momenta over the beam width, and with dodecapole correction windings. After construction and successful operation of a prototype magnet in the laboratory, competitive tenders were obtained from industry on the basis of technical specifications and manufacturing drawings. The magnets proper and the cryostats are being manufactured under two separate contracts. The insertion will be installed within 1980 at intersection I8, for use in physics experiments with a large magnetic spectrometer.

1. Introduction

From the very beginning of colliding beam experimentation at the ISR, studies were carried out on the possible compression of the vertical amplitude functions β of the beams at one particular crossing, by means of quadrupole magnets, in order to increase the luminosity. A low-β insertion using classical quadrupoles was implemented in 1974[1]: it increases the luminosity in its intersection by a factor 2.3.

More powerful focusing insertions[2] were shown to require such high magnetic gradients as could only be achieved in quadrupoles with superconducting windings and high current densities. After successful construction and operation of a prototype of such a quadrupole[3], the construction of a complete high-luminosity insertion[4] was approved in 1977. In July 1978, it was decided that the insertion should be installed at intersection I8, for use with a large axial magnetic field spectrometer. Only the final configuration, adapted to this specific application, is described in this paper.

In addition to its usefulness for physics experimentation, the project has a twofold technical interest: on one hand, it is the first attempt to insert superconducting magnets into the beam guiding system of an operating storage ring, on the other hand, the construction of eight superconducting quadrupoles to tight specifications by industrial firms is a significant technological challenge.

2. Beam Optics of the Low-β Insertion

In order to achieve a large reduction of β_V at an intersection, strong magnetic lenses must be placed near the crossing point. The insertion must be matched as well as possible to the unperturbed machine, which means that the functions β_V, β_h and α_p should not change outside the insertion when the magnets of the insertion are excited: this imposes three matching conditions for the functions and three others for their derivatives in each ring. In addition, β_V at the crossing point must be small and its derivative must be zero: one can see that at least eight parameters per ring are needed for a matched insertion. These parameters could be the positions and strengths of four quadrupole lenses in each ring, if they could be chosen freely: in this case, eight quadrupoles in total would be sufficient.

In practice, the minimum distance of the four nearest quadrupoles from the crossing is fixed by the space requirements of the experimental apparatus, and little freedom exists in positioning the four others. Moreover, the physics experiments would profit from a small interaction diamond, so that also α_p and β_h should be made as small as possible at the crossing. Two more quadrupoles were therefore added, in suitable straight sections of the adjacent inner arcs of the machine (Fig. 1), to help with the matching procedure.

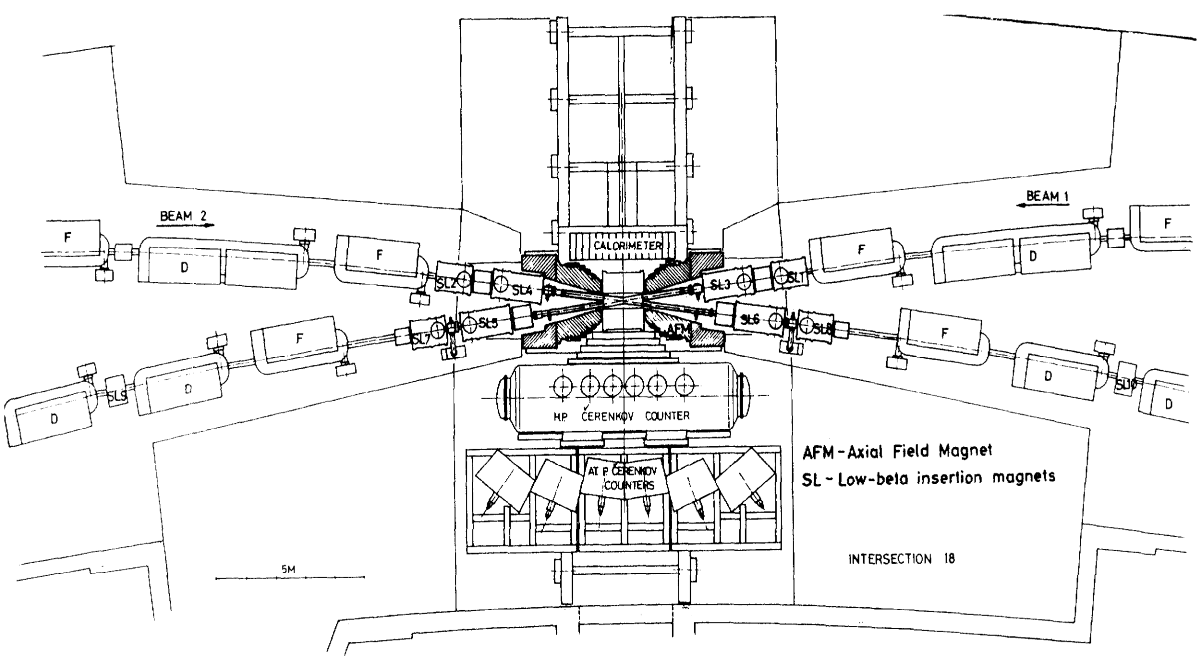

Fig. 1 Layout of the Superconducting High-Luminosity Insertion at Intersection I8

ISR Division, CERN
CH-1211 Geneva-23

0018-9499/79/0600-3179$00.75 © 1979 IEEE

The gradients of the main ISR magnets were adjusted, at the start, so that the phase advances produced by the insertion would push the working line into the so-called ELSA region of the stability diagram (immediately below the main diagonal, and centred on $Q_h = 8.90$, $Q_v = 8.88$), where low order resonances can be avoided and the ISR are most successfully operating with high currents and low background for experiments.

The ISR must operate with a positive chromaticity in order to provide Landau damping of the transverse coherent instability. Therefore, sextupoles must be added inside the superconducting quadrupoles in order to match the off-momentum particle orbits. The quadrupole and sextupole strengths of the magnets are given in Table 1. Table 2 shows the beam optics parameters with the low-β insertion.

TABLE 1

Parameters of the low-β insertion magnets

Name		SL1 SL2	SL3 SL4	SL5 SL6	SL7 SL8	SL9 SL10
Technology		SC	SC	SC	SC	clas-sical
Polarity		F	D	D	F	F
Quadrupole magnetic length	[m]	0.65	1.15	1.15	0.65	0.385
Quadrupole gradient	$[\mathrm{T\,m^{-1}}]$	39.9	42.7	37.75	37.9	5.33
Sextupole magnetic length	[m]	0.74	1.24	1.24	0.74	0
Sextupole gradient derivative	$[\mathrm{T\,m^{-2}}]$	13.6(1) 11.5(2)	21.4	21.4	24.1	0

The matching of the insertion is good in β_v and α_p, but poor in β_h, for which the maximum value outside the insertion, at the top of the stack, is 183.4 m, almost a factor 4 larger than in the unperturbed machine. The increase of the horizontal betatron amplitudes reduces the available momentum bite in the stack, However, this reduction is not too prejudicial to the luminosity if the beam intensity is vacuum limited. The effective beam height at the low-β crossing is reduced by a factor 6.4, and the luminosity gain, with respect to the unperturbed machine, is expected to be between 5 and 6.

The fact that the maxima of β_h and α_p are reached outside the insertion is advantageous, because it reduces the background for the experiments and the disturbance to the superconducting quadrupoles due to radial beam losses.

The width and length of the interaction diamond at the low-β intersection are reduced by a factor 2.5 with respect to the normal machine.

3. The Superconducting Quadrupoles

In order to allow normal operation of the ISR when the low-β insertion is not excited, the quadrupoles must accommodate a machine vacuum chamber at least 150 mm wide and its bakeout jacket. Their warm bore must therefore be at least 173 mm. The other parameters of the quadrupoles (see Table 1) are determined by beam optics and cryogenic requirements.

Figure 2 shows two sections of a quadrupole in its cryostat. The conductor of the main coils is a solid composite wire of rectangular cross-section

TABLE 2

Beam optics parameters with the low-β insertion on ELSA line

	Parameters		At central orbit $\Delta p/p = 0$	At extreme orbit $\Delta p/p = 0.0176$
outside the insertion	α_p^{max}	[m]	2.299	2.437
	β_v^{max}	[m]	57.209	55.561
	β_h^{max}	[m]	118.127	183.228
	β_v^{min} at any intersection	[m]	14.864	12.946
in the insertion	β_h^{max}	[m]	70.908	99.086
	β_v^{max}	[m]	66.178	60.777
	α_p^{max}	[m]	2.241	2.417
at low-β crossing	β_v	[m]	0.293	0.319
	β_h	[m]	2.728	1.638
	α_p	[m]	1.050	1.119

β_v in normal machine [m] 12.238

1.8 × 3.6 mm, containing about 1250 twisted NbTi filaments, 50 μm in diameter, inside a copper matrix. It is insulated with enamel and polyimide tape. Each coil has 290 turns, continuously wound in three quasi-rectangular blocks on a central stainless steel post, and spaced by copper wedges of suitable width to approximate a cos 2θ current distribution. The coil ends have a constant perimeter profile, which eases winding under tension. Each coil is individually moulded and vacuum-impregnated with epoxy resin.

The four coils are wrapped together with glass-epoxy bands, to form a compact self-supporting cylinder, which is able to withstand the large precompression applied by the steel quadrants when the aluminium rings shrink strongly onto them at cooldown. Thanks to the prestress, the coils do not suffer or deform under the action of the electromagnetic forces, and the magnet can perform satisfactorily. Two full scale prototype magnets have operated repeatedly and reproducibly at a gradient of 45 $\mathrm{T\,m^{-1}}$, with a current of 1680 A and a maximum field of 5.8 T, and have shown no retraining after repeated warmups and cooldowns. When pulsed up to quench, they were able to absorb, without damage, their stored energy of 700 kJ.

The sextupole windings are made of solid rectangular enamelled conductor of 1.3 × 0.7 mm, which has to carry 220 A in order to produce the maximum required sextupole component of 24.1 $\mathrm{T\,m^{-1}}$. They are located in grooves in the wall of the inner tube of the helium vessel and precompressed by means of epoxy silica wedges wrapped by aluminium alloy wire under strong tension. Other grooves contain the dodecapole correction windings.

The magnet and the helium vessel, which is welded around it, are suspended in the vacuum tank of the cryostat by means of Inconel bands attached to their ends.

Magnetic measurements, performed in the warm bore of the prototype cryomagnet, have shown the gradient in-

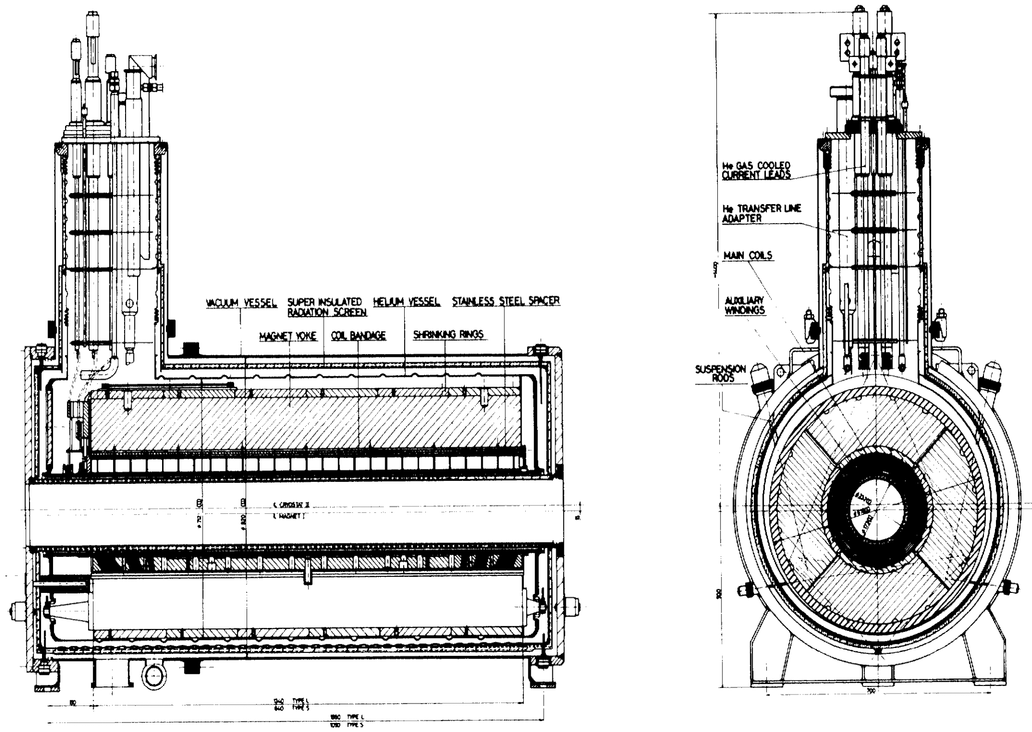

Fig. 2 Longitudinal and Transverse Sections of a Quadrupole in its Cryostat

tegrals to be correct to within 10^{-3}, which is the required tolerance, over the useful aperture. The helium consumption of the prototype was found to be 13 l h^{-1}, of which 8 in the leads.

4. Construction Progress and Installation Planning

One of the purposes of the project is the transfer of superconducting technology to European industry. Therefore, a considerable amount of work was invested into the preparation of detailed specifications and manufacturing drawings, in order to make it possible for firms to evaluate the costs in terms of ordinary production standards and to submit competitive tenders. A very positive response was obtained, which permitted to place, before the end of 1977, the four major contracts, namely those for the superconducting wire, the manufacturing of the quadrupoles proper, the cryostats and the refrigeration plant.

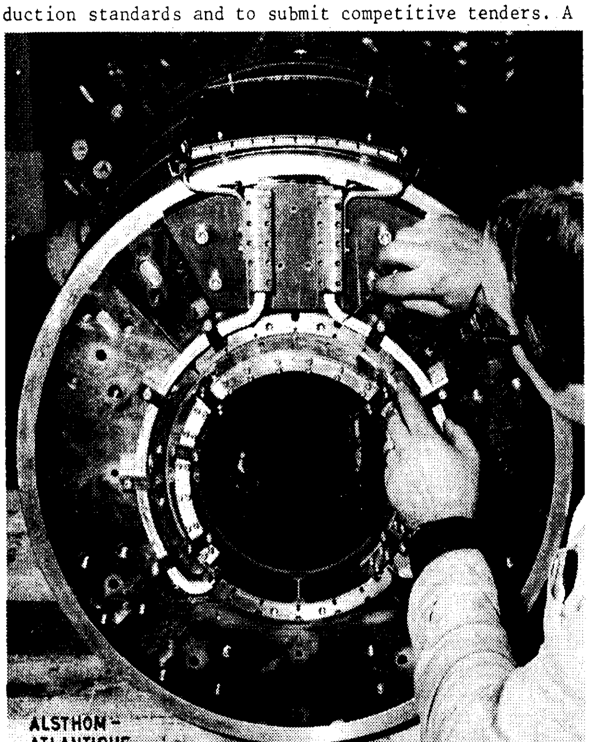

Fig. 3 The First Finished Quadrupole at the Factory

The first quadrupole has already been delivered, assembled into its cryostat, tested and measured with satisfactory results. Figure 3 shows the first quadrupole ready for delivery to CERN.

The insertion will be located at intersection I8, where an experiment to study large transverse momentum phenomena in both pp and $p\bar{p}$ collisions will be run. The experimental equipment consists of an axial-field magnet (AFM) surrounded by a set of detectors. The two nearest quadrupoles to the crossing will have to be located partly inside the conical poles of the AFM. The resulting layout of intersection I8 is shown in Fig. 1.

The liquefier and the power supplies have to be located outside the ISR tunnel. The cryogenic transfer lines will be 50 m long and will run in a labyrinth through the tunnel wall. Flexible transfer lines[5] with vapour-cooled screens were developed for this purpose. Their losses are $\sim$0.05 W m^{-1}. Individual transfer lines for the cryostats will preserve the operational independence of the quadrupoles. The eight quadrupoles and their auxiliary windings must also be individually powered.

References

1. J.P. Gourber, E. Keil, S. Pichler, The first high-luminosity insertion in the ISR, IEEE Tractions on Nuclear Science, Vol. NS-22, No. 3, p.1419 (June 1975).

2. B. Autin, Région d'intersection à faible β_V dans les ISR, Div. Report CERN ISR-MA/72-45 (1972).

3. J. Billan et al., Construction of a prototype superconducting quadrupole magnet, Report CERN 76-16 (1976).

4. A. Verdier, Revised superconducting low-β scheme for the ISR, Div. Report CERN ISR-BOM/77-57 (1977).

5. H. Laeger et al., Long flexible transfer lines for gaseous and liquid helium, Cryogenics, Vol. 18, No. 12, p. 659 (Dec. 1978).